Abdominal Radiology

Published online: 1 October 2018

Abdom Radiol (2019) 44:1535–1553
https://doi.org/10.1007/s00261-018-1784-9

Fatty masses of the abdomen and pelvis and their complications

Monica R. Drylewicz,[1] Meghan G. Lubner,[2] Perry J. Pickhardt,[2] Christine O. Menias,[3] and Vincent M. Mellnick[1]

[1]Washington University in St. Louis, St. Louis, MO, USA
[2]University of Wisconsin, Madison, WI, USA
[3]Mayo Clinic, Scottsdale, AZ, USA

Abstract

There are numerous common and rare macroscopic fat-containing masses found in the abdomen and pelvis. These include benign masses, such as lipoleiomyoma, ovarian teratoma, mesenteric teratoma, and lipoma, as well as malignant masses, including liposarcoma and malignant transformation of benign entities. Any mass may become symptomatic due to the development of a complication which may range from ovarian torsion to intussusception to hemorrhage. Imaging plays a vital role in diagnosis and treatment planning when confronted with a symptomatic fat-containing mass.

Key words: Fat-containing—Teratoma—Fatty—Lipoma

Abdominopelvic masses containing macroscopic fat are encountered on an almost daily basis by abdominal imagers, often incidentally. These masses include benign lesions, such as mature cystic teratoma, lipoleiomyoma, lipoma, angiomyolipoma, and myelolipoma, and malignant lesions, such as liposarcoma, hepatocellular carcinoma, and malignant degeneration of a benign mass [1–4].

Though many fat-containing masses are benign, a variety of complications may be seen secondary to its presence in the abdomen or pelvis. This may result in the patient presenting to their physician or emergency department. Such complications include ovarian torsion, pain, hemorrhage, and bowel obstruction. Herein, we describe a number of macroscopic fat-containing masses of the abdomen and pelvis which were discovered due to symptoms related to a complication.

Correspondence to: Monica R. Drylewicz; *email:* astrisize@gmail.com

Imaging plays a vital role in identification of a cause for a patient presenting symptom(s). It can narrow the differential diagnosis of a fat-containing mass based on its features or even definitively diagnose a mass [5]. CT is the workhorse for evaluation of presenting symptoms due to its wide availability and rapid rendering of diagnostic images. MR may often be used in those patients who are less ideal candidates for CT (pregnancy, young age, mild renal insufficiency) as well as for further characterization of masses previously identified on CT or US.

Computed tomography identifies macroscopic fat as an area/structure of low attenuation with a Hounsfield value less than fluid, generally in the range of − 10 to − 100 [5]. Microscopic fat is less readily obvious on CT, and MR techniques are more sensitive in detection [6]. On magnetic resonance imaging, fat is hyperintense on T1 and T2 and may be suppressed by multiple techniques including inversion-recovery and chemically selective fat suppression. Chemical shift artifact can also help to identify the border between fat and soft tissue/fluid or to identify microscopic fat. [7] The vital role imaging plays in diagnosis and directing treatment is highlighted.

Fatty masses

Mature cystic teratoma

An often asymptomatic and incidentally identified fat-containing mass in the pelvis is the mature cystic teratoma of the ovary or dermoid cyst [8, 9]. This mass is most common during the reproductive years though can occur at any age and account for 10–20% of ovarian neoplasms. The mature cystic teratoma is a cystic tumor composed of at least two of the three germ cell layers. Adipose tissue is present in approximately 3/4 of these masses. Teeth, bone, and hair may also be present within the mass. At CT, fat attenuation of the sebaceous cyst component with soft tissue calcifications may be seen. Often, a protuberance is seen projecting into a sebaceous

cystic cavity and is termed the Rokitansky nodule. This appearance is virtually pathognomonic. On US, the so-called "tip of the iceberg" sign may be seen in which the echogenic sebum, hair, and/or calcifications result in marked posterior acoustic attenuation. This obscures the rest of the mass thus rendering recognition of the true size impossible. On MR, high T1 and T2 signal indicative of macroscopic fat is present and confirmed with loss of signal upon fat suppression. In contradistinction, immature teratomas of the ovary comprise less than 1% of ovarian teratomas and are primary malignant lesions made up of all three germ cell layers [9].

A variety of complications may be found secondary to the presence of this mass, most presenting with a complaint of pelvic pain. CT or US is most often ordered upon initial presentation for the identification of the cause of pain. Further evaluation may then be pursued as desired by the treating physician or surgeon. Ovarian torsion is the most common complication of a mature cystic teratoma (Fig. 1). The risk of torsion increases with the size of the mass. Rupture of the sebaceous cystic cavity may also occur and result in pain and possibly chemical peritonitis (Fig. 2). Malignant degeneration, though rare, is also a recognized complication and occurs in 0.2–2% [7, 10]. The most commonly encountered malignancy arising from a mature cystic teratoma is squamous cell carcinoma (Fig. 3). When encountered incidentally, follow-up is recommended if the mass is not surgically resected [11].

Lipoleiomyoma

A rare form of the more commonly encountered uterine leiomyoma or fibroid is the lipoleiomyoma, a mass of the uterus which contains not only fibrous tissue and smooth muscle, but also fat. The incidence is low, ranging from 0.03 to 0.2% [12] and is more common in postmenopausal women. Presenting symptoms may include pain, palpable pelvic mass, or abnormal uterine bleeding. On ultrasound, a heterogeneous hyperechoic mass may be seen in the uterus. On CT, areas of low attenuation representing fat and areas of intermediate attenuation representing soft tissue including muscle and fibrous tissue are identified. On MR, the mass is heterogeneous with areas of T1/T2 hyperintensity representing fat. The soft tissue areas of the mass demonstrate the enhancement on CT and MR (Fig. 4).

These masses are benign and treatment is guided by symptoms. If discovered incidentally and the patient remains asymptomatic, no treatment is generally recommended. If symptomatic, uterine artery embolization, resection, or hysterectomy may be recommended based on an individual patient's presentation, symptoms, and desires with special consideration in patients desiring future fertility. The malignant form of this mass, lipoleiomyosarcoma, is exceedingly rare [12, 13].

Mature cystic teratoma of the mesentery

A mass similar in appearance to an ovarian mature cystic teratoma may also rarely form in the mesentery [14] or retroperitoneum [15]. This lesion demonstrates similar imaging features as those encountered in the adnexa. In a case series, fat was present in 60% of retroperitoneal teratomas [15]. In the mesentery, these lesions are more common prior to the 4th decade of life. Patients may present with pain due to the mass itself, mass effect on adjacent organs, or even bowel obstruction (Fig. 5). Resection is the preferred treatment.

Gastrointestinal lipoma

Fat-containing masses or mass-like processes may often be encountered in the bowel. The fat-containing gastrointestinal lipoma is most commonly located in the colon (65–75%) with 90–95% in the submucosa [16]. The peak incidence is in approximately the 5th–7th decade [17]. On CT, a purely fat-containing mass will be seen within the bowel with variable areas of higher attenuation. On MR, the fatty mass will be characteristically high in intensity on T1 and T2 images with fat saturation. Again, this type of mass is often encountered incidentally, either on imaging or colonoscopy. Though possibly worrisome on colonoscopy, the etiology of the mass is often easily identified on imaging given the predictable characteristics [18].

The majority of gastrointestinal lipomas are asymptomatic with risk of complication likely correlating with size [19]. When symptomatic, patients may complain of abdominal pain secondary to intussusception, in which the lipoma serves as the lead point (Fig. 6) [20]. In addition to pain, bright red blood per rectum, melena, or anemia may be the presenting symptom in the case of hemorrhage of the fatty mass (Fig. 7) [21].

Retroperitoneal liposarcoma

Retroperitoneal liposarcoma is the most common primary malignant tumor arising from the mesenchyme with variable differentiation. In fact, a fat-containing mass arising from the retroperitoneum (as opposed to the kidney or adrenal gland) should be considered liposarcoma until proven otherwise, often surgically [22]. The malignancy is slightly more common in men than women with peak incidence around age 50. They are very rare in children. Most are well differentiated. These lesions may grow to be quite large given the potential space in the retroperitoneum and exert mass effect on the surrounding organs. On CT, low attenuation fat in the retroperitoneum is present with variable amounts of soft tissue. MR demonstrates similar findings with high T1/T2 signal intensity with mixed in variably sized areas of higher attenuation which may enhance.

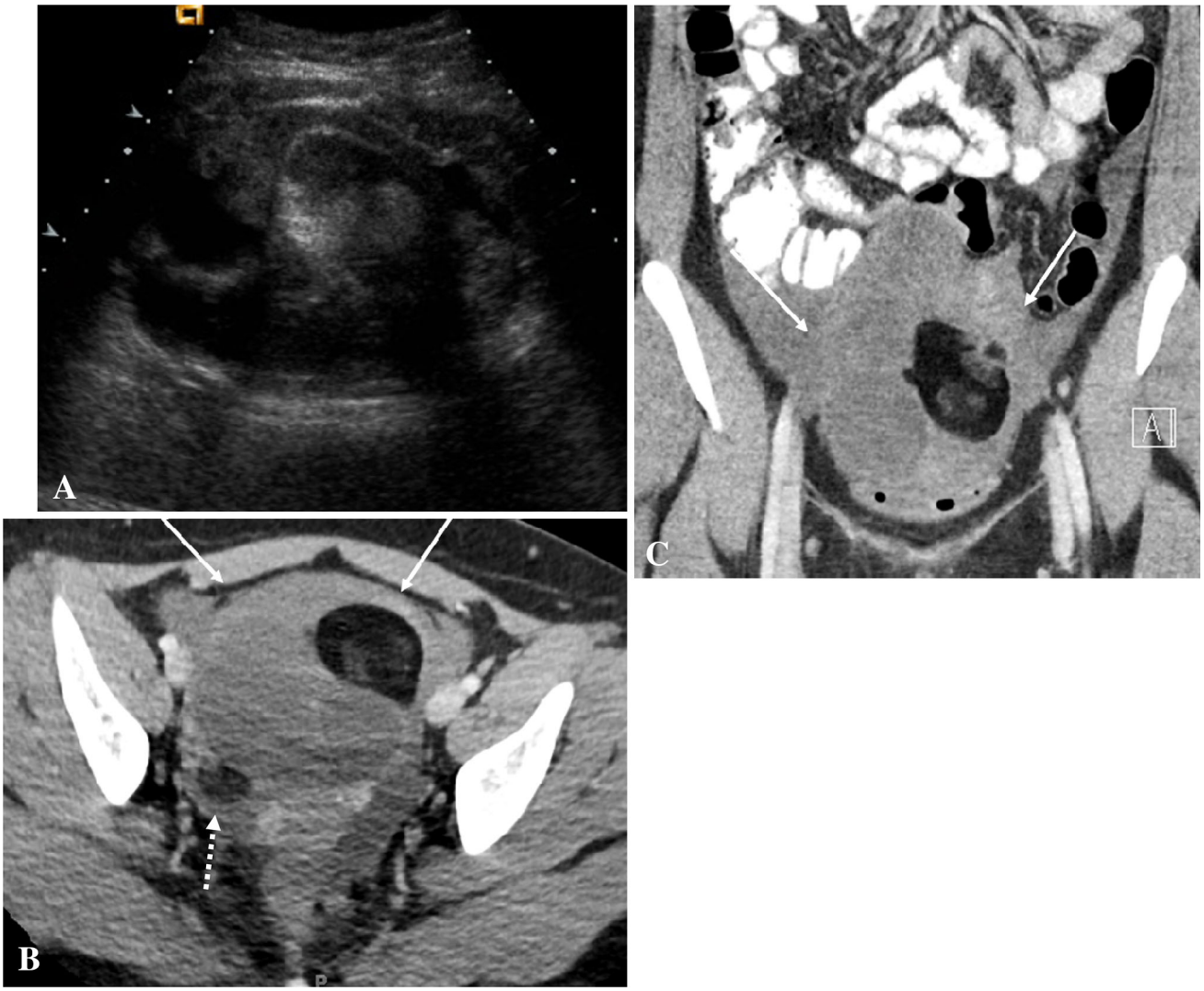

Fig. 1. Torsion of a left ovarian mature cystic teratoma: a 16-year-old female patient presents with pelvic pain. **A** Initial ultrasound demonstrates a complex midline mass containing hyperechoic and hypoechoic components. **B**, **C** Axial and coronal CT images show a fat-containing mass with soft tissue components arising from the left adnexa (white arrows). Free fluid is also noted in the pelvis. The patient was taken to surgery for concern for torsion which confirmed torsion secondary to ovarian mature cystic teratoma. Incidentally, a small right ovarian mature cystic teratoma is also present but without complication (dashed arrow in **B**).

Patients may present with symptoms of pain (Fig. 8) or other complications such as obstruction. Differential diagnoses for retroperitoneal liposarcoma include causes of increased fat within the retroperitoneum. These include retroperitoneal lipomatosis and HIV-associated lipodystrophy (Fig. 9) [5, 23]. These processes are bilateral and more symmetric in appearance though differentiation from a well-differentiated liposarcoma with minimal soft tissue may be quite challenging.

Truly, lipoma and liposarcoma may be encountered virtually anywhere within the abdomen and pelvis and differentiation between benign and malignant is often difficult or impossible on imaging. Both entities are also occasionally encountered in the spermatic cord and can present a challenge in identification in the setting of inguinal hernia. These masses may cause hernia-like symptoms (Fig. 9) but will not be alleviated by hernia repair. It is an important consideration in addressing fat-containing processes of the inguinal canal and close attention to anatomic landmarks may help in differentiation. [24]

Angiomyolipoma

Angiomyolipomas (AML) arise from the renal cortex and are the most common mass categorized as a PEComa or perivascular epithelioid cell tumor. Such tumors are mesenchymal neoplasms made up of smooth


A
B
C
D

◀**Fig. 2.** Ovarian mature cystic teratoma rupture: a 25-year-old female presents with pelvic pain. **A** Axial CT images demonstrate a large primarily fat-containing mass with calcifications and small soft tissue components consistent with ovarian mature cystic teratoma. **B** The wall of the mass has ruptured with fat stranding indicative of inflammation near the site of rupture (dashed arrow) and small fatty deposits (white arrows). **C**, **D** Additional axial images demonstrate fatty deposits (arrows) throughout the pelvis consistent with rupture.

muscle and melanocytic cells. [25, 26] AMLs are seen in approximately 0.3–3% of the population with the majority occurring sporadically (90%). The mass is more common in females than males (2:1) [27]. When multiple and/or bilateral, there is often an underlying genetic predisposition of tuberous sclerosis. On imaging, a mass within the retroperitoneum is present and may be demonstrated as renal in origin by a claw sign in which the renal cortex forms an obtuse angle with the mass [5].

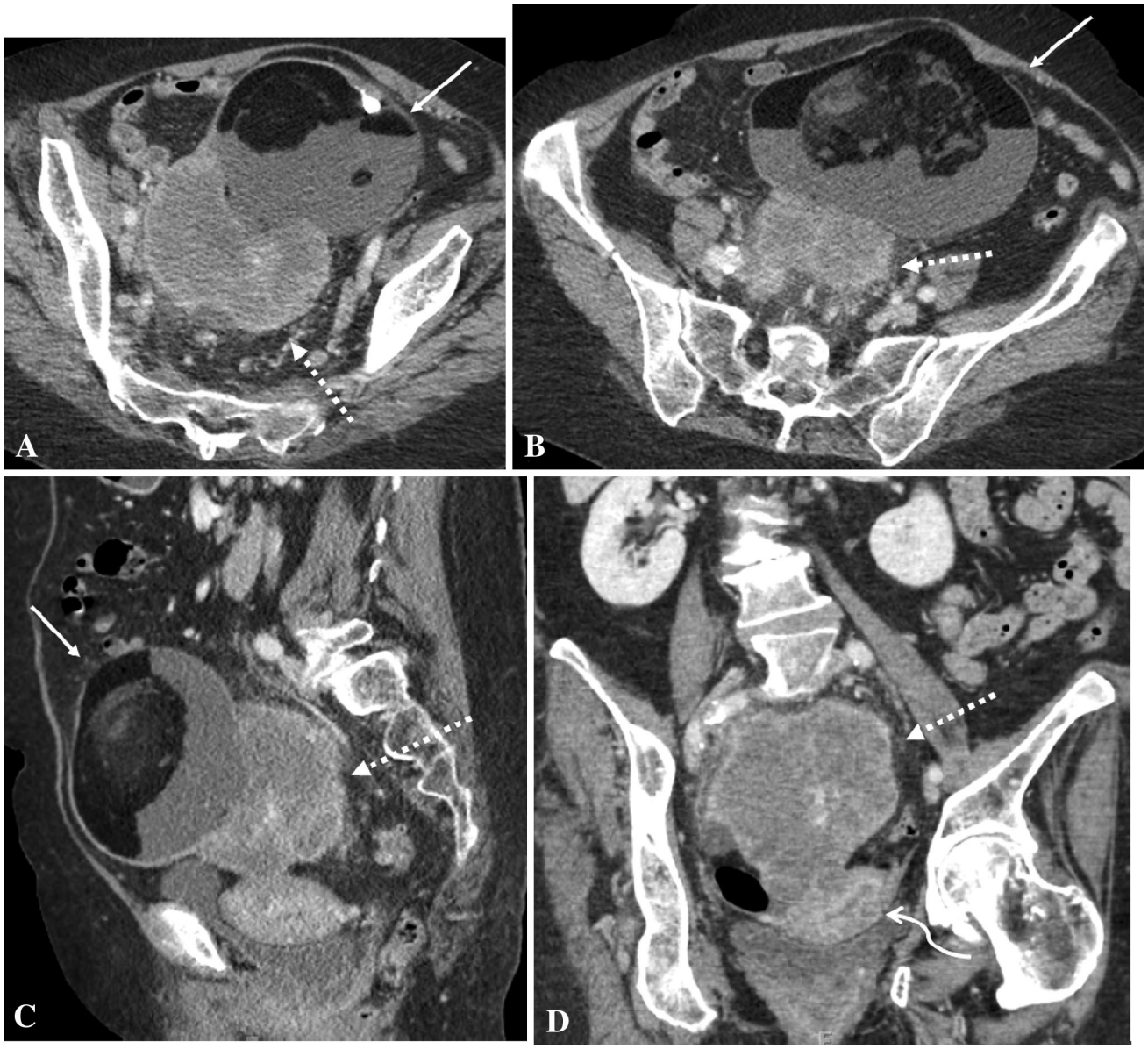

Fig. 3. Malignant transformation of an ovarian teratoma: a 72-year-old female presents with pelvic pain. **A**–**D** Axial (**A**, **B**), sagittal (**C**), and coronal (**D**) images demonstrate a large mass of mixed fat, solid tissue, fluid, and calcium components (white arrows) consistent with a mature cystic teratoma. Posteriorly, there is an irregular enhancing solid mass (dashed arrows) concerning for malignant transformation of the teratoma. **D** On the coronal image, there is mass effect upon the uterus with deviation leftward (curved arrow) suggesting the origin of the mass to be the right adnexa. Upon right oophorectomy, pathology demonstrated squamous cell carcinoma arising in a mature cystic teratoma.

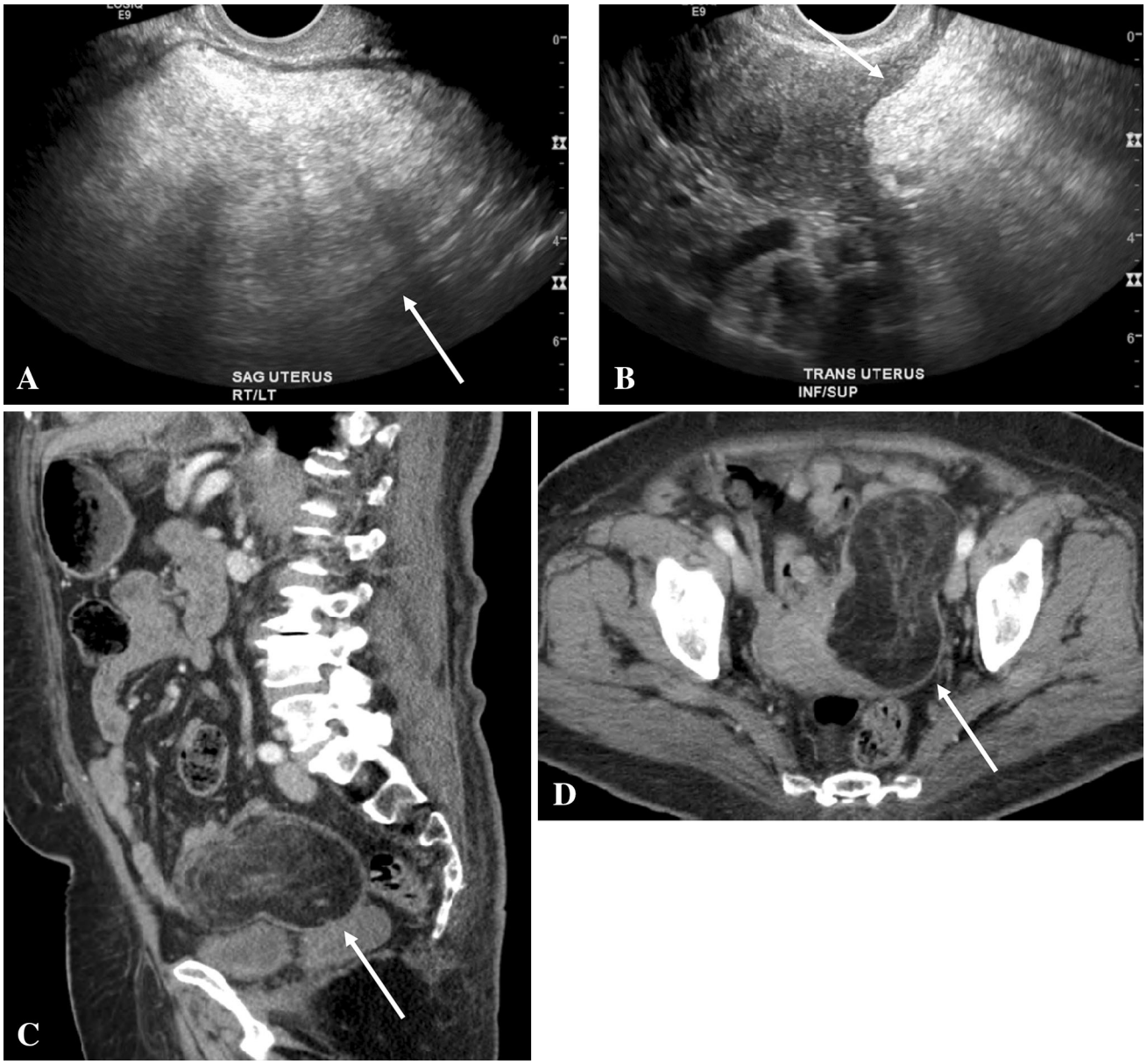

Fig. 4. Lipoleiomyoma: a 56-year-old female presents with pelvic pain. **A**, **B** On ultrasound, a large hyperechoic mass (arrows) is closely associated with the uterus with mass effect on the organ. **C**, **D** Sagittal (**C**) and axial (**D**) CT images demonstrate a predominately fat-containing mass (arrows) arising from the right of the uterus with a mild amount of soft tissue attenuation. Given the proximity to the adnexa, a mature cystic teratoma may be considered. The findings may also represent an atypical lipoma, liposarcoma, or lipoleiomyoma. Surgical pathology following resection demonstrated lipoleiomyoma without malignant features.

On ultrasound, the mass is homogeneously hyperechoic. On CT, the mass demonstrates low attenuation equivalent to the surrounding retroperitoneal fat with variable amounts of soft tissue. Tortuous arterial vessels may be appreciated on arterial CT imaging or angiography. High T1/T2 signal intensity is present on MR which will demonstrate loss of intensity with fat suppression. When macroscopic fat is present, the mass can be confidently diagnosed on imaging.

There are also many recognized, though rare, AMLs with atypical findings. The most common of these is the lipid poor AML, which comprises approximately 5% of AMLs and may be indistinguishable from renal cell carcinoma, which may require resection for final diagnosis. Another variant of AML harbors malignant potential itself, known as the epithelioid AML. This mass resembles a renal cell carcinoma on imaging with aggressive features as well as the ability to invade the renal vein and inferior vena cava [28].

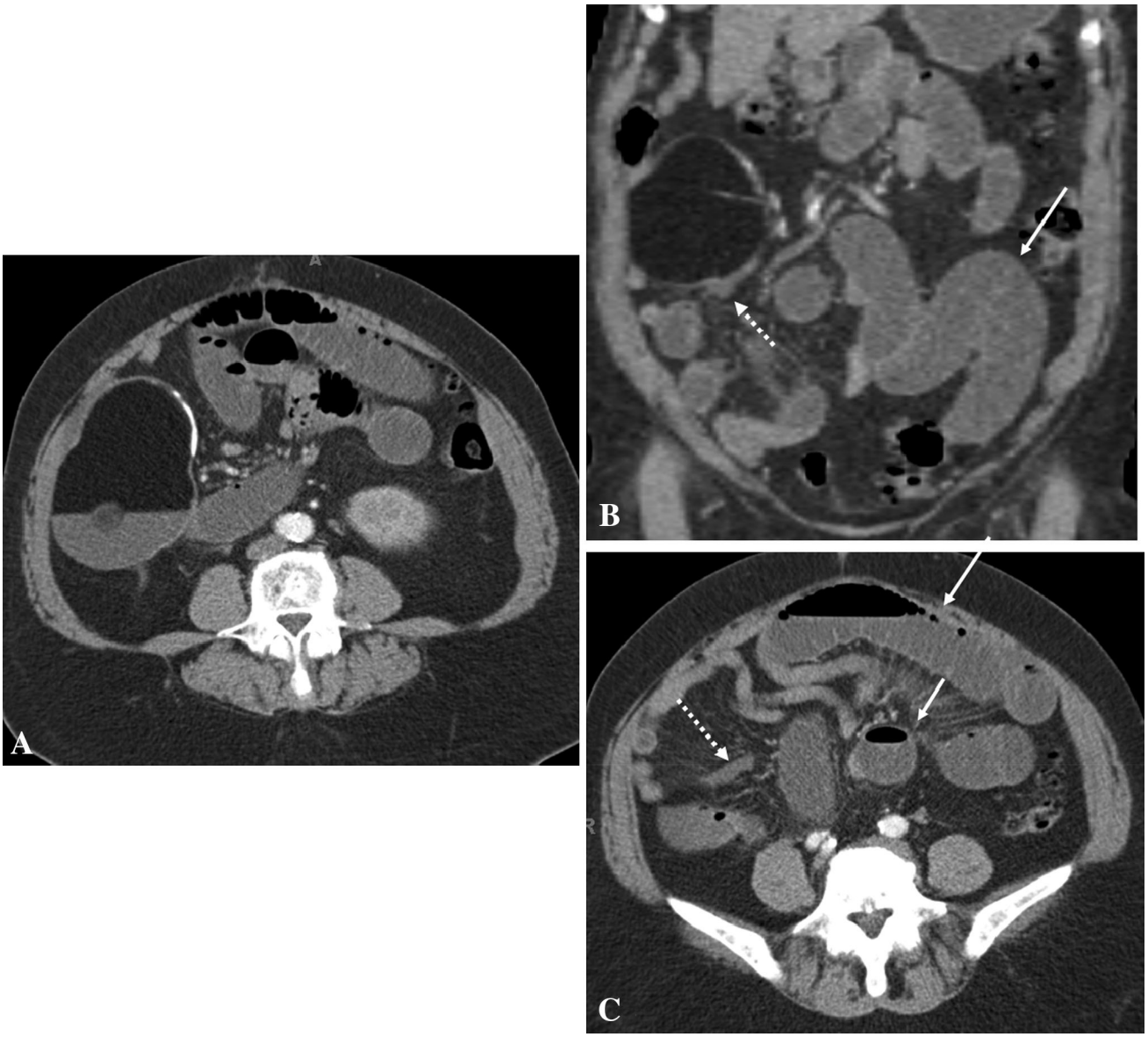

Fig. 5. Small bowel obstruction secondary to mesenteric teratoma: an 80-year-old female presents with abdominal pain. **A** Axial CT images demonstrate a large primarily fat-containing mass with peripheral calcifications and fat-fluid level consistent with mesenteric teratoma. **B**, **C** Coronal reconstruction (**B**) and additional axial image (**C**) demonstrate multiple dilated loops of small bowel (white arrows) with a transition point at the mass and segment of decompressed bowel adherent to the inferior aspect of the mass (dashed arrows). After failing conservative management, the patient was taken to surgery for resection.

The most common complication of AML is hemorrhage, often presenting with pain, shortness of breath, or loss of consciousness. This potentially life-threatening complication is most commonly treated with embolization by an interventional radiologist in the acute setting (Fig. 10). Resection may be performed to prevent hemorrhage in larger masses, often recommended at > 4 cm [29].

AMLs are a common manifestation in patients with tuberous sclerosis [30], occurring in 55–75% of affected patients. When encountered in tuberous sclerosis, AMLs are more often multiple, larger, bilateral, encountered at a younger age, and likely to grow.

Adrenal myelolipoma

Another fat-containing mass within the retroperitoneum is the adrenal myelolipoma. This entity is rare with a prevalence of 0.08–0.4% [31]. There is no gender predilection. Myelolipoma is a benign fat-containing mass which arises from the adrenal gland and demonstrates varying amounts of hematopoietic tissue [32]. On

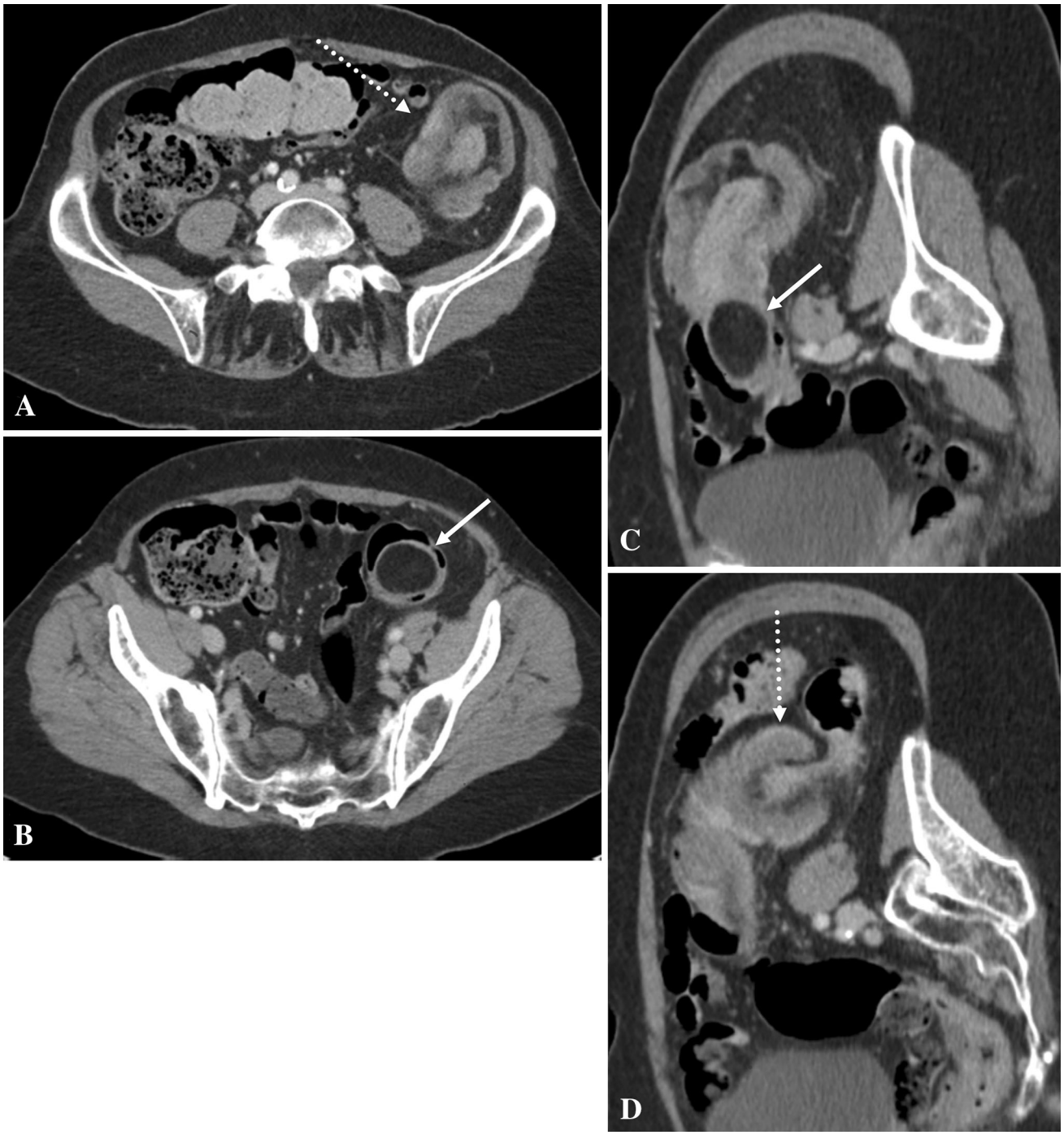

Fig. 6. Intussusception from colonic lipoma: a 61-year-old female presents with abdominal pain. **A** Colocolic intussusception (dashed arrow) is identified in the left lower quadrant involving the descending and sigmoid colon. **B** A lead point fat-containing mass is identified consistent with benign lipoma (white arrow). **C**, **D** Multiplanar reformatted images were created to better demonstrate the lead point lipoma (white arrow, **C**) and proximal portion (dashed arrow, **D**) of the intussusception well. Left colectomy was performed. Pathology confirmed pedunculated submucosal lipoma without evidence of dysplasia or malignancy.

CT, the adrenal mass contains low attenuation areas representing macroscopic fat within the often predominantly soft tissue mass. On MR, high T1/T2 signal intensity is present with decreased signal on fat suppression. India ink artifact on opposed-phase imaging representing a border between fat and soft tissue/fluid can often be helpful in identifying small deposits of macroscopic fat. Though these lesions are benign,

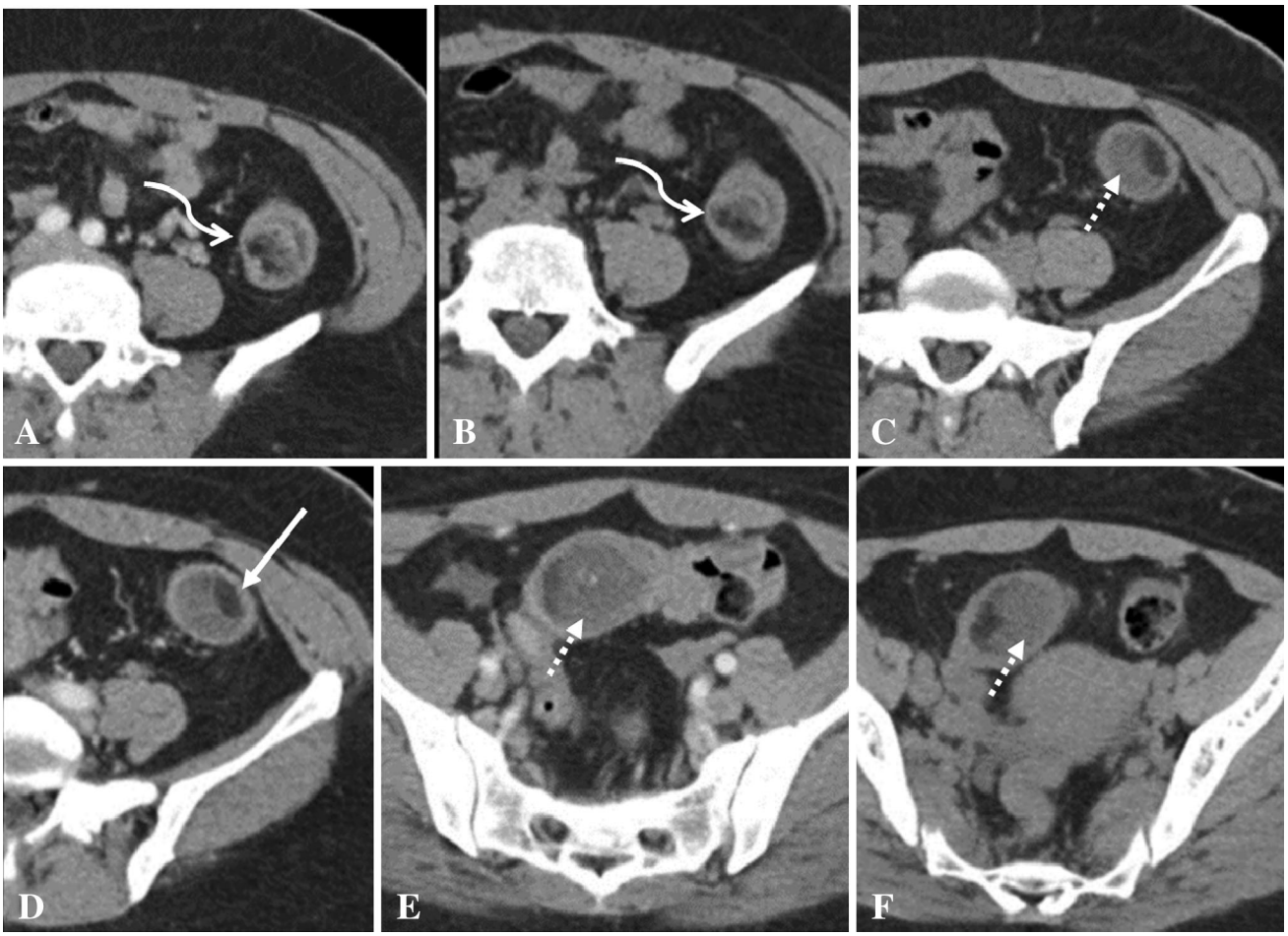

Fig. 7. Bleeding colonic lipomatosis: a 43-year-old female presents with bright red blood per rectum. **A**–**F** Axial CT images of the descending and sigmoid colon demonstrate multiple fatty masses consistent with lipomas (white arrow). Some show internal high attenuation consistent with hemorrhage (curved arrows) with a large amount of high attenuation material in the colon (dashed arrows) representing blood products, confirmed by colonoscopy and surgery.

definitive diagnosis may require resection if the imaging is equivocal and cannot differentiate the mass from a retroperitoneal lipoma/liposarcoma.

The most common complication of adrenal myelolipoma is hemorrhage which generally presents similarly to hemorrhage of renal angiomyolipoma. This event may require vascular intervention or surgery for management (Fig. 11) [33]. The occurrence of hemorrhage in myelolipoma is generally low. One review demonstrated an overall spontaneous hemorrhage rate of 17.1% in tumors greater than 6 cm [34].

Hepatocellular carcinoma

Though presence of microscopic fat is more common, macroscopic fat may be found in the most common primary malignancy of the liver, hepatocellular carcinoma. The tumor is strongly associated with cirrhosis from alcohol and/or hepatitis viral infections as well as increasingly due to nonalcoholic steatohepatitis [35]. The diagnosis may be made on the basis of well-defined imaging criteria alone within a cirrhotic liver including lesion size and growth, arterial phase hyperenhancement, washout, and pseudocapsule [35]. These criteria may obviate the need for biopsy and the associated risks, such as hemorrhage (Fig. 12).

Other common and uncommon fat-containing liver masses include adenoma, hepatic adrenal rest tumor, angiomyolipoma, and pseudolipoma of Glisson's capsule (Fig. 13) [1, 2]. Hepatic adenomas are relatively common masses containing hepatocytes with various amounts of adipose. They are differentiated pathologically based on genetics which confer prognostic information [1]. Full discussion of this entity is outside the scope of this review. The hepatic adrenal rest tumor is an ectopic mass of adrenocortical cells located within the liver, most commonly in the subcapsular right liver [1]. Angiomyolipoma of the liver also displays a variable amount of

macroscopic fat, many of which lack obvious fat content. The majority of these lesions are sporadic but a small percentage (< 10%) are seen in association with renal AMLs in the setting of tuberous sclerosis [30]. The pseudolipoma of Glisson's capsule is another rarely encountered fat-containing liver mass located along the hepatic capsule. It is thought to represent a detached and migrated epiploic appendage which formed a fibrous capsule and is attached to the liver capsule [1].

Normal fat-containing structures

Fat is normally present in a number of structures throughout the abdomen and pelvis. These masses or mass-like processes too can become symptomatic, generally due to ischemia and resultant inflammation and/or necrosis [36]. The role of imaging of these structures and complications is important in demonstrating their benign nature allowing for conservative management.

The omentum is a fold of peritoneum composed of fat extending from the stomach and covering the visceral abdominal organs. If blood flow is impeded to a portion

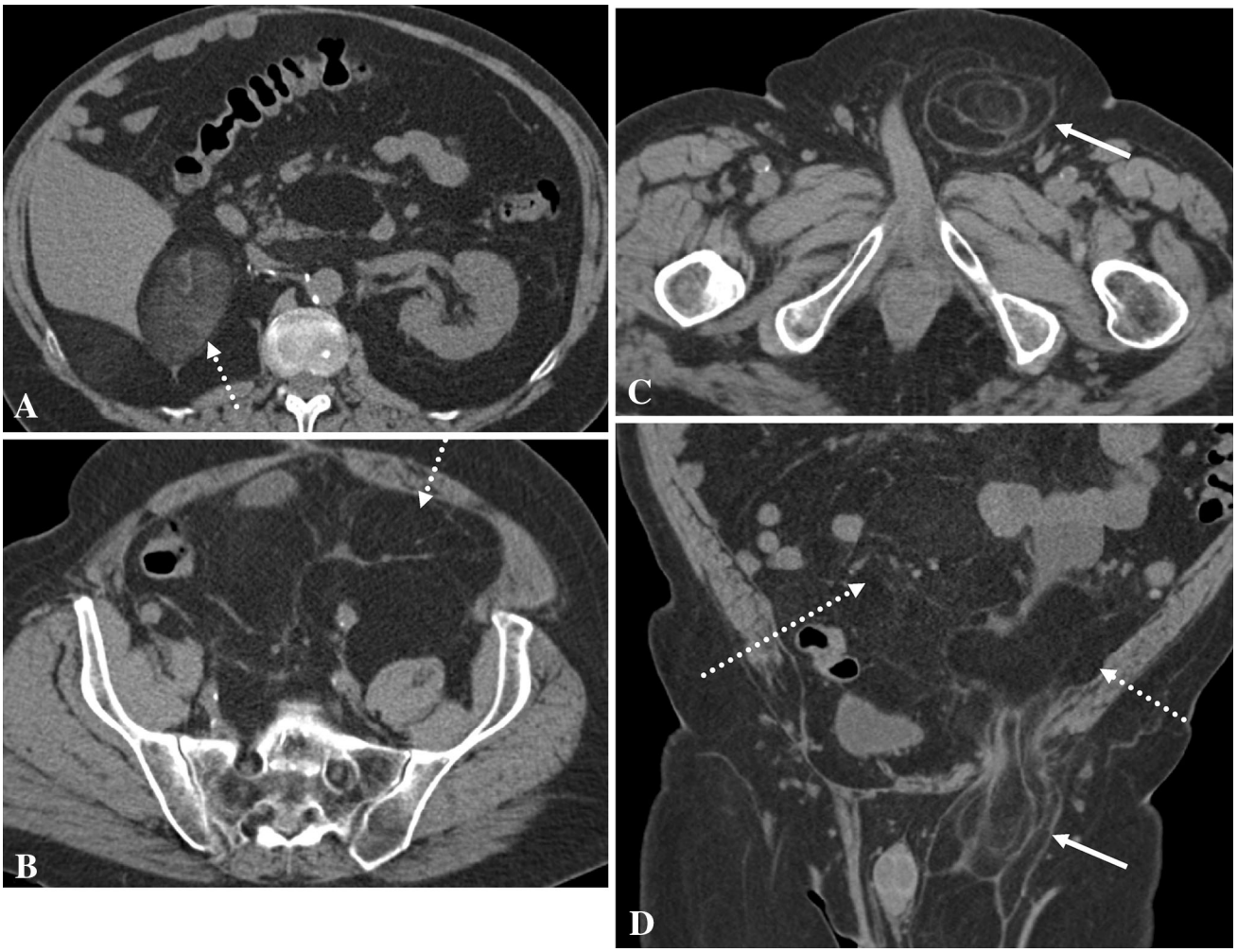

Fig. 8. Inguinal hernia containing retroperitoneal liposarcoma: a 74-year-old male with history of large retroperitoneal liposarcoma status post resection presented with severe scrotal pain. **A**–**D** Axial (**A**–**C**) and coronal (**D**) CT images demonstrate widespread recurrence of liposarcoma evidenced by fat- and soft tissue-containing masses (dashed arrows) in the right retroperitoneum (**A**), left pelvis (**B**), and mesentery (**D**) with extension of the mass through the left inguinal canal (white arrow, **C**, **D**). Due to the severity of the patient's symptoms, he was taken to the OR for palliative bulk resection.

Fig. 9. Differential diagnoses for retroperitoneal and inguinal liposarcoma: **A**, **B** Retroperitoneal lipomatosis is seen on fat-saturated T2-weighted axial imaging (**A**) as well as coronal T2-weighted imaging (**B**). **C**, **D** An HIV positive patient on antiretroviral therapy was imaged with incidental note of marked increase in retroperitoneal fat with minimal peripheral subcutaneous fat consistent with HIV-associated lipodystrophy. **E**, **F** A 61-year-old male presented with right inguinal hernia. Biopsy of the fatty mass surrounding the spermatic cord (arrow) of the right inguinal canal confirmed liposarcoma.

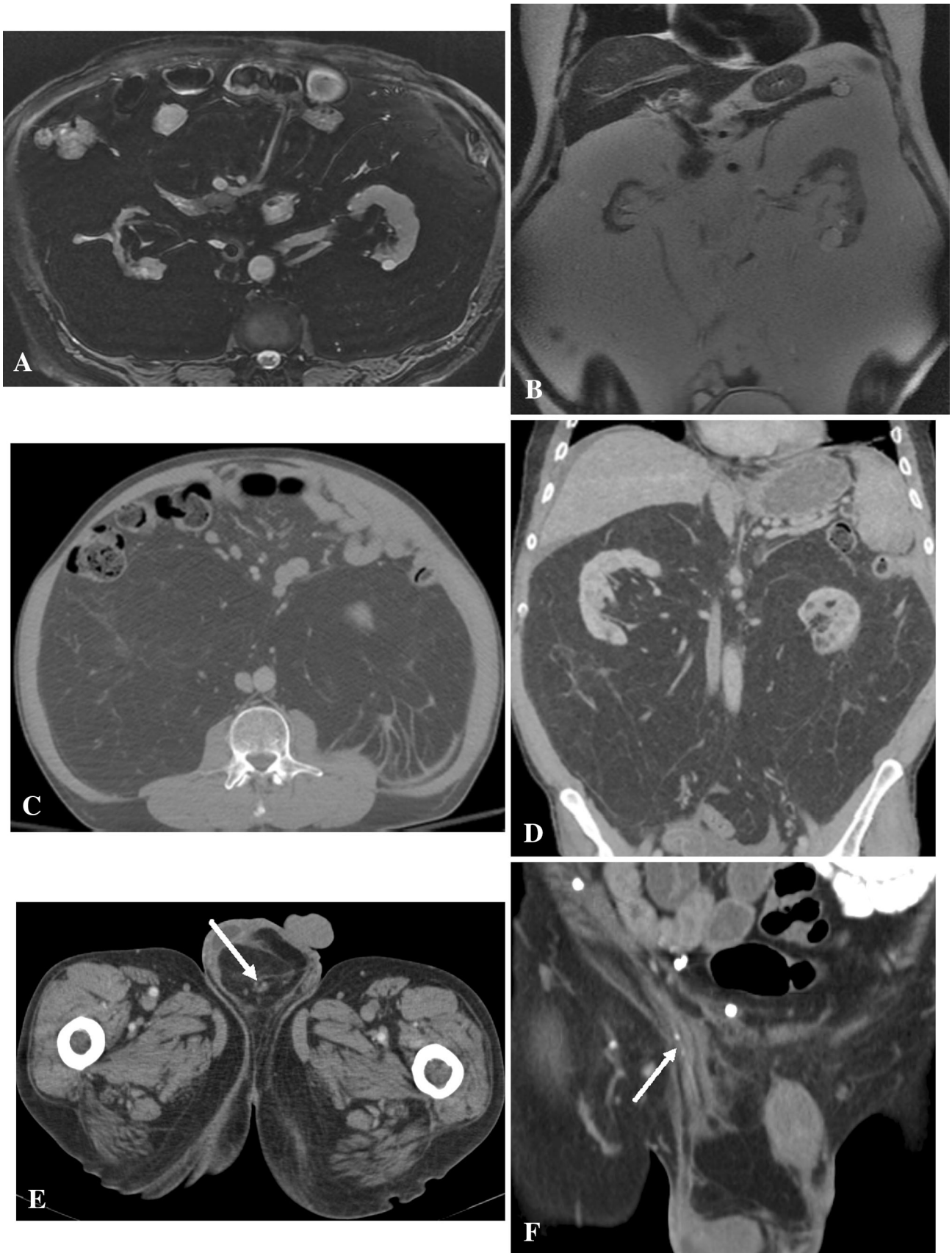
A
B
C
D
E
F

of the omentum by torsion or thrombosis, an infarct may occur resulting in patient complaint of pain. Fat necrosis may be encountered postoperatively. Imaging demonstrates a focus of fat surrounded by soft tissue stranding within the anterior abdomen (Fig. 14). Diagnosis of omental infarct by imaging allows for confident treatment of the patient's pain without follow-up or surgery required.

Another normal fat-containing structure in the abdomen is the epiploic appendage, a focus of subserosal fat arising from the surface of the large bowel and lined by peritoneum. These are often not visible on imaging as they are indistinct from the surrounding peritoneal fat though they may occasionally be visible due to the presence of ascites or contrast. Torsion or thrombosis may occur and cause ischemia and inflammation which is termed epiploic appendagitis (Fig. 15). This condition can cause a large amount of pain but requires no treatment other than symptomatic pain relief. Thus, its diagnosis by CT or MR is crucial to avoid unnecessary intervention.

The fatty appendage of the falciform ligament, another fat-containing fold of the peritoneum, is also not generally visible on cross-sectional imaging until torsion

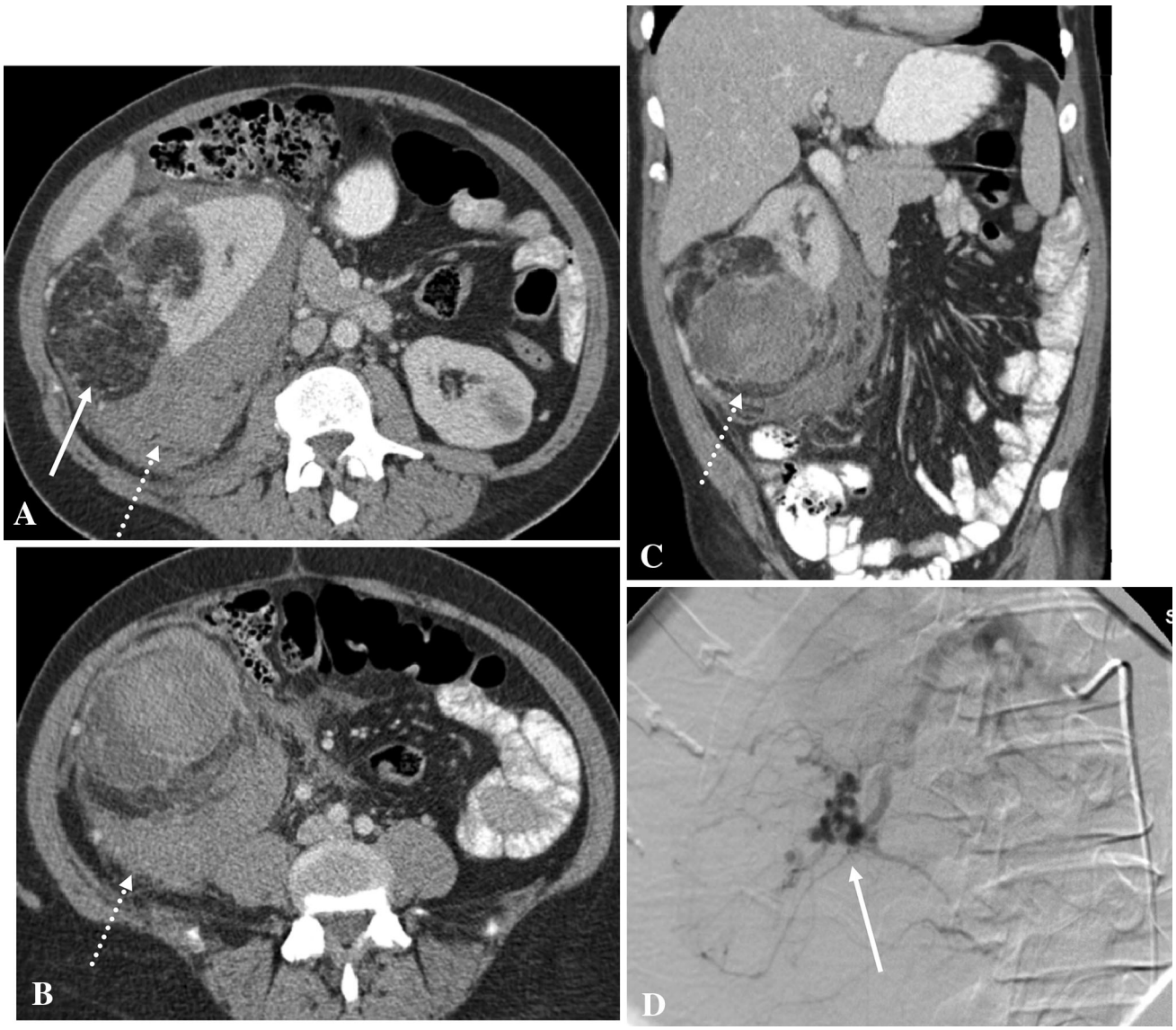

Fig. 10. Rupture and hemorrhage of a renal angiomyolipoma: a 45-year-old female presented with severe right flank and back pain. **A**–**C** Axial (**A**, **B**) and coronal (**C**) CT images demonstrate a large mixed attenuation mass (arrow) arising from the right kidney with right retroperitoneal hemorrhage (dashed arrows). A cyst is noted in the left kidney. **D** Angiography confirmed a large vascular renal mass (arrow) consistent with hemorrhage of an angiomyolipoma. Ethanol ablation and coil embolization of the feeding artery was successful and follow-up imaging 2 months later (not shown) confirmed decreased size of the mass and hemorrhage.

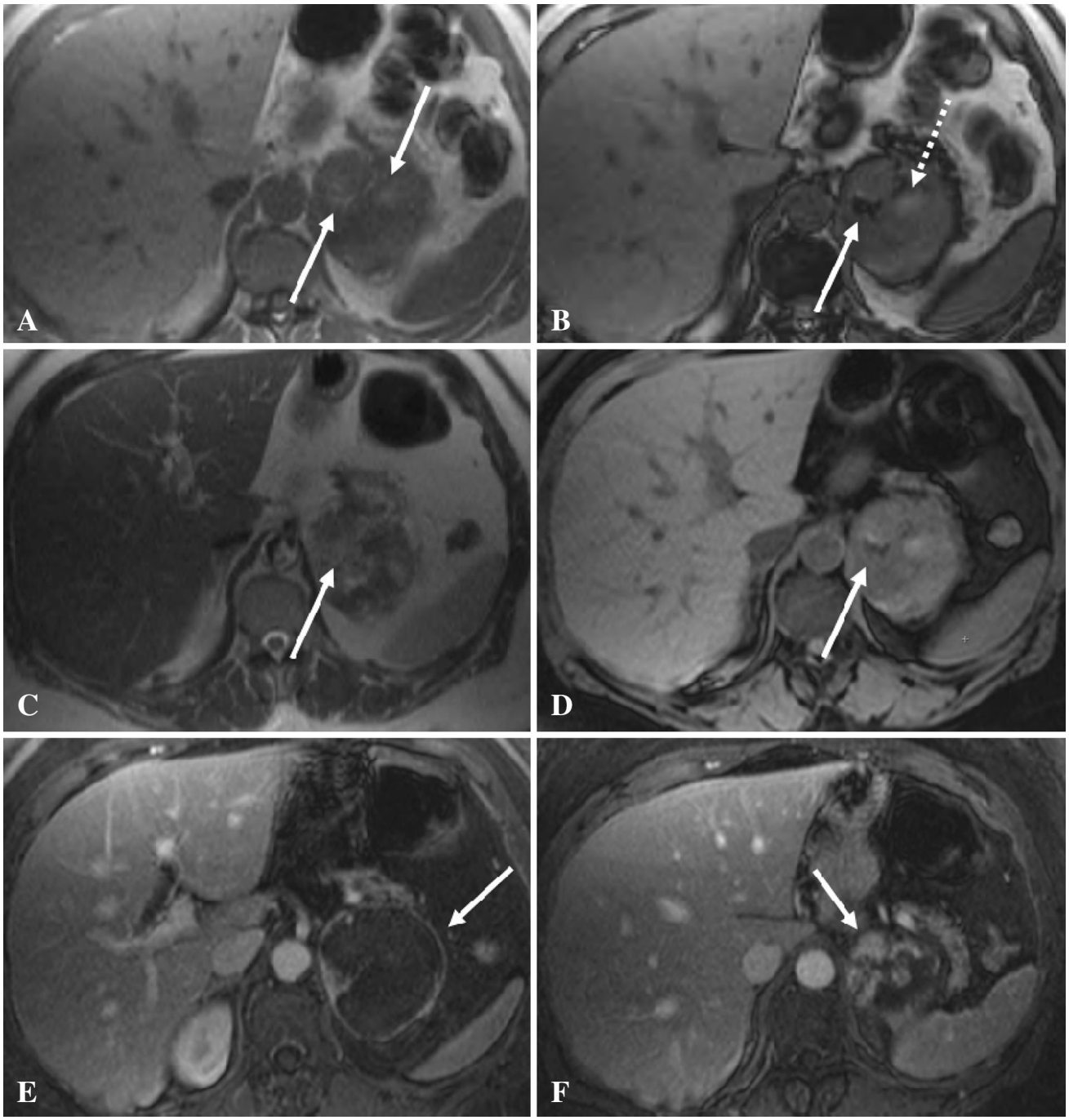

Fig. 11. Hemorrhage within adrenal myelolipoma: a 70-year-old female presented for follow-up MRI for a large left adrenal mass. **A** In-phase imaging demonstrates multiple areas of high T1 signal intensity (white arrows). **B** Opposed-phase imaging at the same axial level shows India ink artifact surrounding one area consistent with the presence of macroscopic fat (white arrow). The second area of high T1 intensity is likely hemorrhage or proteinaceous material (dashed arrow). **C**, **D** T2-weighted imaging (**C**) also demonstrates high signal intensity (arrow) in the first area in A which drops on fat-saturated TrueFISP imaging, most consistent with macroscopic fat given all the described signaling characteristics. **E**, **F** Post-contrast imaging predominately demonstrates rim enhancement (arrow, **E**) but areas of more nodular enhancement superiorly (arrow, **F**). Due to interval growth, the mass was resected. Pathology demonstrated benign adrenal myelolipoma with hemorrhage.

Fig. 12. Fat-containing hepatocellular carcinoma with hemorrhage: A 63-year-old male presented with growing liver mass. **A**, **B** Pre-contrast (**A**) and arterial phase (**B**) axial CT images demonstrate a vascular mass with nodular internal enhancement (white arrows) which may have predisposed the patient to hemorrhage following biopsy. **C** On coronal images, the mass also shows at least one focus of macroscopic fat (dashed arrow). **D** Following biopsy for diagnosis, a large amount of hemoperitoneum (white arrows) developed. Pathology confirmed hepatocellular carcinoma.

or ischemia results in surrounding inflammation (Fig. 16). Again, the patient may present with pain but does not require intervention other than pain control.

Conclusion

A variety of fat-containing masses may be found in the abdomen and pelvis either incidentally or secondary to complications of their presence. Most fat-containing masses are benign though some are malignant or have malignant potential. Imaging plays a vital role in discovering these masses, defining their characteristics, often allowing for confident diagnosis without percutaneous biopsy or surgical resection, and identifying any complications to plan appropriate targeted management, which may be conservative or invasive.

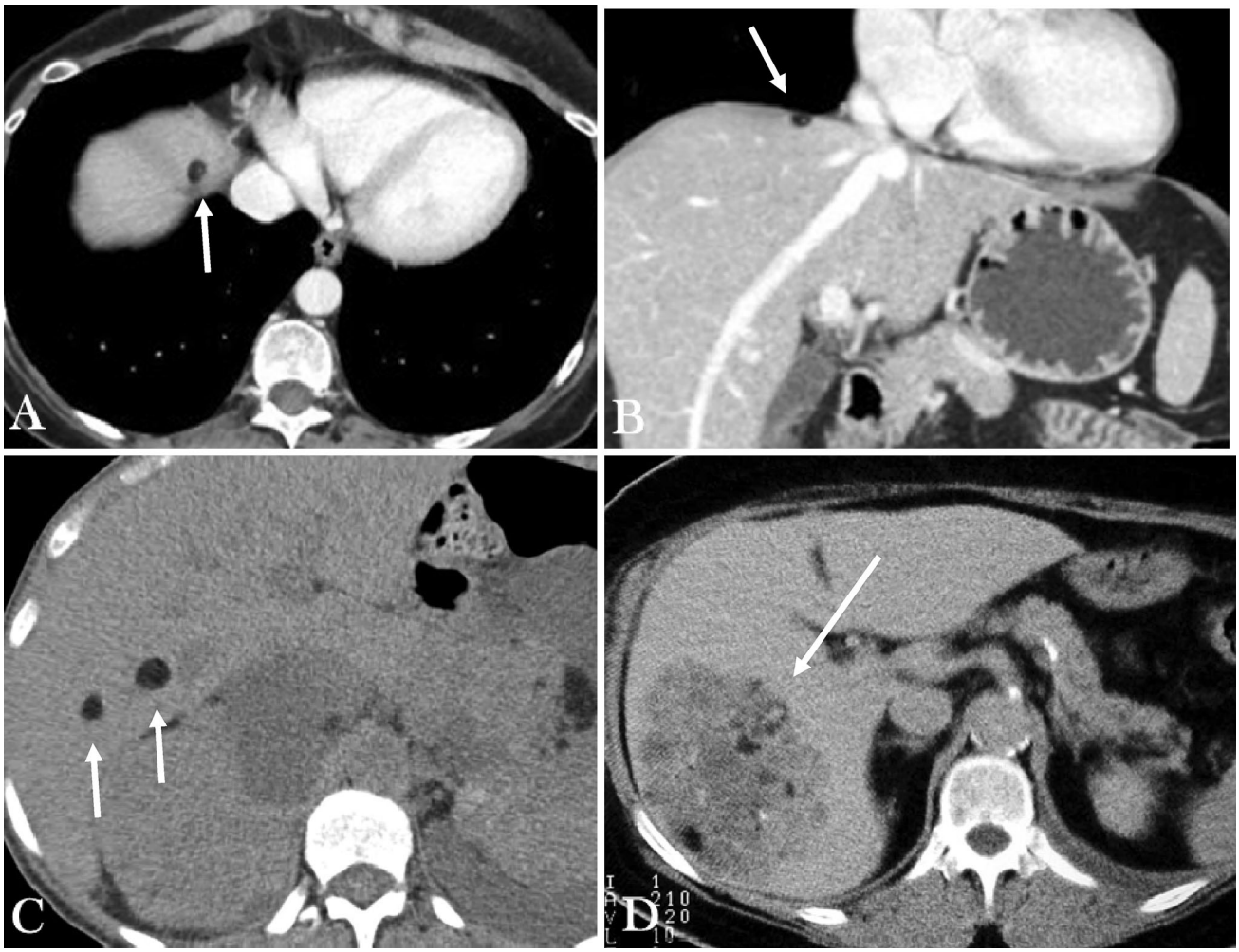

Fig. 13. Other fat-containing hepatic lesions: **A**, **B** Pseudolipoma of Glisson's capsule (arrows) is shown on axial (**A**) and coronal (**B**) CT images. **C** Two small angiomyolipomas of the liver (arrows) are demonstrated in a patient with tuberous sclerosis. **D** A heterogeneous mass (arrow) in the right liver extending from the capsule with macroscopic fat is consistent with hepatic adrenal rest tumor.

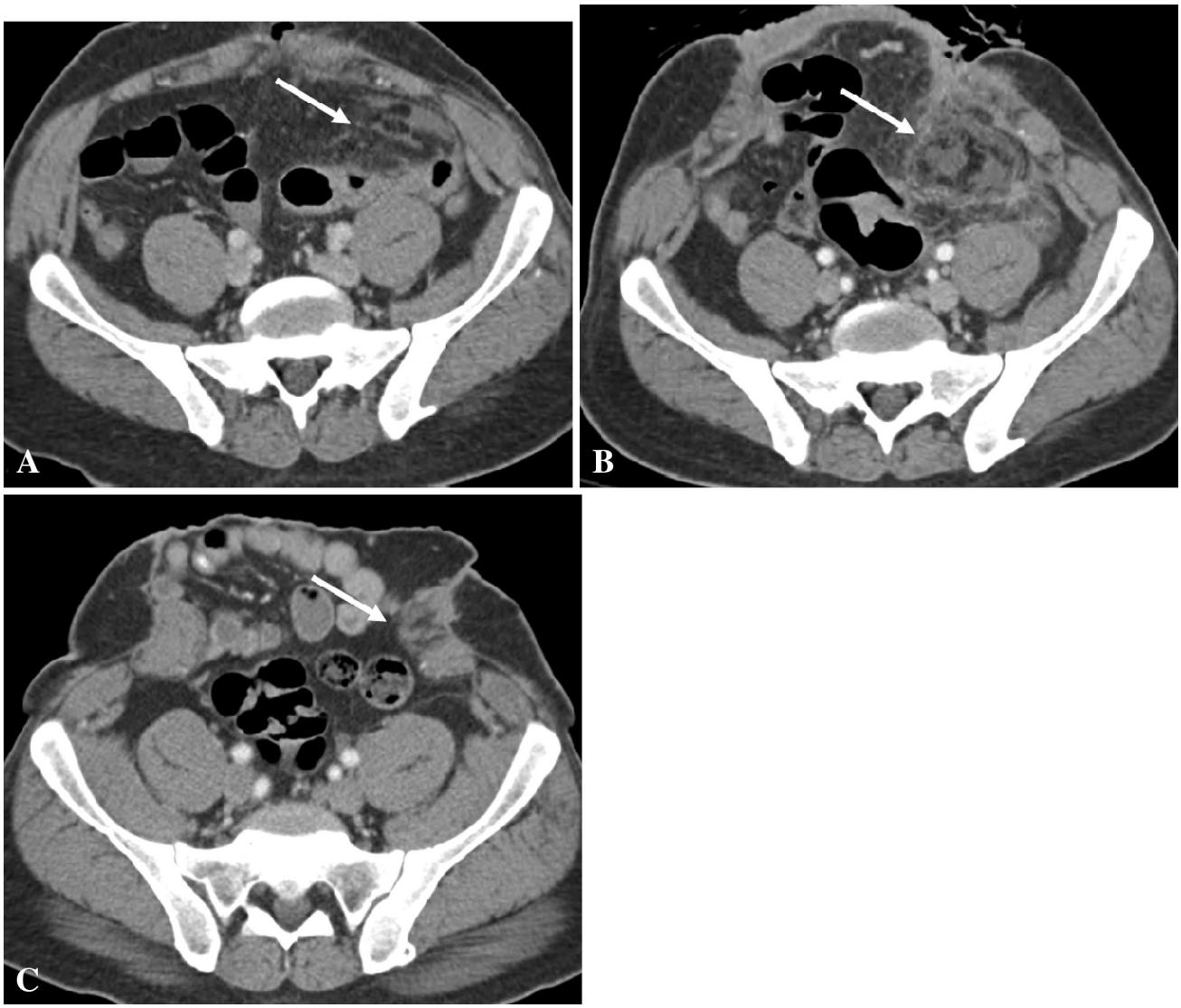

Fig. 14. Omental fat infarct: a 42-year-old male presented following gun shot with wound dehiscence. **A** Initial CT shows high density fluid in the left lower quadrant surrounding fat (arrow). **B** Follow- up one month later shows increased organization of the left lower quadrant collection with soft tissue density surrounding fat (arrow) consistent with fat necrosis/omental infarct. **C** Imaging one year later shows resolution of the omental infarct (arrow).

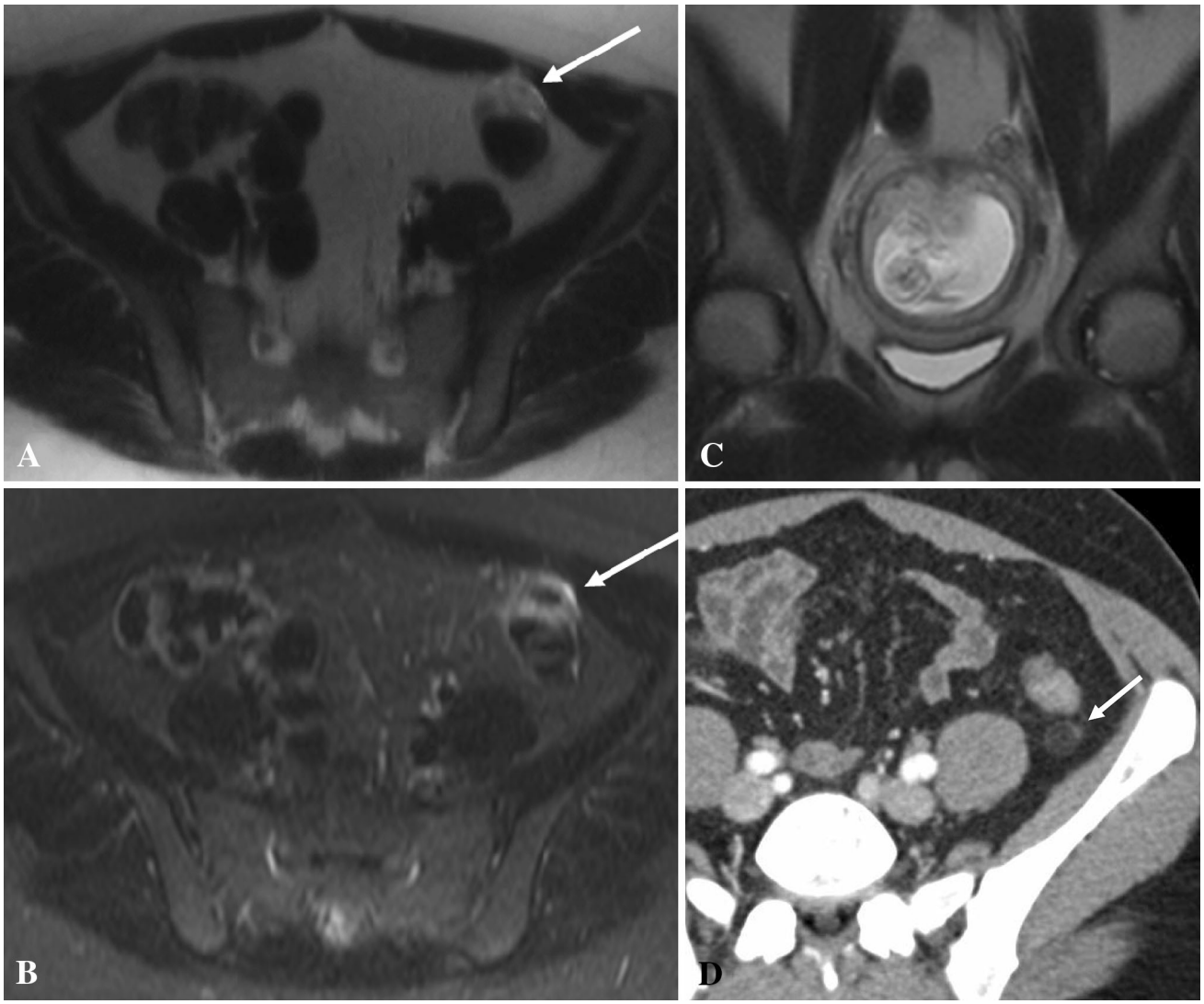

Fig. 15. Epiploic appendagitis: A 32-year-old pregnant female presented with left lower quadrant abdominal pain. MRI was performed to spare radiation exposure to the pregnant patient and fetus. **A**, **B** T2-weighted (**A**) and T2 fat-saturated (**B**) axial MRI images demonstrate inflammation surrounding an oval collection of fat—evidenced by loss of signal on the fat-saturated image—directly adjacent to the descending colon (arrows) consistent with epiploic appendagitis. **C** Coronal T2-weighted image shows the intrauterine pregnancy. The patient was treated conservatively for pain. **D** Similar findings are also demonstrated on CT with stranding surrounding a rounded area of fat attenuation (arrow) adjacent to the descending colon, also consistent epiploic appendagitis.

Fig. 16. Torsion of the fatty appendage of the falciform ligament: a 72-year-old female presents with new abdominal pain. **A** Axial CT image shows a normal appearing falciform ligament superiorly (arrow). **B**, **C** Axial images obtained more caudally show stranding of the fat surrounding the falciform ligament (arrows). **D** This stranding is best appreciated on sagittal CT imaging through the midline which demonstrates the extent of soft tissue attenuation/fat stranding associated with the falciform ligament as it courses inferiorly. These findings are most consistent with fat necrosis of the fatty appendage of the falciform ligament. The patient was treated conservatively and symptoms improved.

Compliance with ethical standards

Funding This study received no funding.

Conflict of interest MD, CM, and VM have no disclosures. ML has received grant funding from Philips and Ethicon. PP serves as an advisor to Bracco, is a shareholder in SHINE, Elucent, and Cellectar.

References

1. Prasad SR, Wang H, Rosas H, et al. (2005) Fat-containing lesions of the liver: radiologic-pathologic correlation. Radiographics 25:321–331
2. Basaran C, Karcaaltincaba M, Akata D, et al. (2005) Fat-containing lesions of the liver: cross-sectional imaging findings with emphasis on MRI. AJR Am J Roentgenol 184:1103–1110
3. Dodd GD 3rd, Budzik RF Jr (1990) Lipomatous tumors of the pelvis in women: spectrum of imaging findings. AJR Am J Roentgenol 155:317–322
4. Black JD, Roque DM, Pasternak MC, et al. (2015) A series of malignant ovarian cancers arising from within a mature cystic teratoma: a single institution experience. Int J Gynecol Cancer 25:792–797
5. Shaaban AM, Rezvani M, Tubay M, et al. (2016) Fat-containing retroperitoneal lesions: imaging characteristics, localization, and differential diagnosis. Radiographics 36:710–734
6. Haider MA, Ghai S, Jhaveri K, Lockwood G (2004) Chemical shift MR imaging of hyperattenuating (>10 HU) adrenal masses: does it still have a role? Radiology 231:711–716
7. Pokharel SS, Macura KJ, Kamel IR, Zaheer A (2013) Current MR imaging lipid detection techniques for diagnosis of lesions in the abdomen and pelvis. Radiographics 33:681–702
8. Multani J, Kives S (2015) Dermoid cysts in adolescents. Curr Opin Obstet Gynecol 27:315–319

9. Outwater EK, Siegelman ES, Hunt JL (2001) Ovarian teratomas: tumor types and imaging characteristics. Radiographics 21:475–490
10. Gershenson DM (2018) Ovarian germ cell tumors: pathology, clinical manifestations, and diagnosis. In: Falk SJ (ed) *UpToDate*. Waltham, MA: Wolters Kluwer
11. Levine D, Brown DL, Andreotti RF, et al. (2010) Management of asymptomatic ovarian and other adnexal cysts imaged at US: society of radiologists in ultrasound consensus conference statement. Radiology 256:943–954
12. Avritscher R, Iyer RB, Ro J, Whitman G (2001) Lipoleiomyoma of the uterus. AJR Am J Roentgenol 177:856
13. McDonald AG, Dal Cin P, Ganguly A, et al. (2011) Liposarcoma arising in uterine lipoleiomyoma: a report of 3 cases and review of the literature. Am J Surg Pathol 35:221–227
14. Papakonstantinou E, Iavazzo C, Hasiakos D, et al. (2011) Extraovarian mature cystic teratoma of the mesentery. A case report and literature review. Clin Exp Obstet Gynecol 38:291–293
15. Davidson AJ, Hartman DS, Goldman SM (1989) Mature teratoma of the retroperitoneum: radiologic, pathologic, and clinical correlation. Radiology 172:421–425
16. Taylor AJ, Stewart ET, Dodds WJ (1990) Gastrointestinal lipomas: a radiologic and pathologic review. AJR Am J Roentgenol 155:1205–1210
17. Ouwerkerk HM, Raber GF, Klaase JM (2010) Duodenal lipoma as a rare cause of upper gastrointestinal bleeding. Gastroenterology Res 3:290–292
18. Thompson WM, Kende AI, Levy AD (2003) Imaging characteristics of gastric lipomas in 16 adult and pediatric patients. AJR Am J Roentgenol 181:981–985
19. Nallamothu G, Adler DG (2011) Large colonic lipomas. Gastroenterol Hepatol 7:490–492
20. Grasso E, Guastella T (2012) Giant submucosal lipoma cause colocolonic intussusception. A case report and review of literature. Ann Ital Chir 83:559–562
21. Zografos G, Tsekouras DK, Lagoudianakis EE, Karantzikos G (2005) Small intestinal lipoma as a cause of massive gastrointestinal bleeding identified by intraoperative enteroscopy. A case report and review of the literature. Dig Dis Sci 50:2251–2254
22. Vijay A, Ram L (2015) Retroperitoneal liposarcoma: a comprehensive review. Am J Clin Oncol 38:213–219
23. Andersen O. A characterisation of low-grade inflammation and metabolic complications in HIV-infected patients. Dan Med J 2016; 63.
24. Cabarrus MC, Yeh BM, Phelps AS, et al. (2017) From inguinal hernias to spermatic cord lipomas: pearls, pitfalls, and mimics of abdominal and pelvic hernias. Radiographics 37:2063–2082
25. Martignoni G, Pea M, Zampini C, et al. (2015) PEComas of the kidney and of the genitourinary tract. Semin Diagn Pathol 32:140–159
26. Jinzaki M, Silverman SG, Akita H, et al. (2014) Renal angiomyolipoma: a radiological classification and update on recent developments in diagnosis and management. Abdom Imaging 39:588–604
27. Fittschen A, Wendlik I, Oeztuerk S, et al. (2014) Prevalence of sporadic renal angiomyolipoma: a retrospective analysis of 61,389 in- and out-patients. Abdom Imaging 39:1009–1013
28. Thiravit S, Teerasamit W, Thiravit P (2018) The different faces of renal angiomyolipomas on radiologic imaging: a pictorial review. Br J Radiol 91:20170533
29. Vicente E, Torres YP (2018) Renal angiomyolipomas. In: Sheridan AM (ed) *UpToDate*. Wotham, MA: Wolters Kluwer
30. Umeoka S, Koyama T, Miki Y, et al. (2008) Pictorial review of tuberous sclerosis in various organs. Radiographics 28:e32
31. Ramirez M, Misra S (2014) Adrenal myelolipoma: to operate or not? A case report and review of the literature. Int J Surg Case Rep 5:494–496
32. Lattin GE Jr, Sturgill ED, Tujo CA, et al. (2014) From the radiologic pathology archives: adrenal tumors and tumor-like conditions in the adult: radiologic-pathologic correlation. Radiographics 34:805–829
33. Liu HP, Chang WY, Chien ST, et al. (2017) Intra-abdominal bleeding with hemorrhagic shock: a case of adrenal myelolipoma and review of literature. BMC Surg 17:74
34. Hsu SW, Shu K, Lee WC, Cheng YT, Chiang PH (2012) Adrenal myelolipoma: a 10-year single center experience and literature review. Kaohsiung J Med Sci 28:377–382
35. Elsayes KM, Hooker JC, Agrons MM, et al. (2017) 2017 version of LI-RADS for CT and MR imaging: an update. Radiographics 37:1994–2017
36. Lubner MG, Simard ML, Peterson CM, et al. (2013) Emergent and nonemergent nonbowel torsion: spectrum of imaging and clinical findings. Radiographics 33:155–173